JOURNAL OF APPLIED ELECTROCHEMISTRY 20 (1990) 223–230

Nucleation and growth of anodic films on stainless steel alloys
I. Influence of minor alloying elements and applied potential on passive film growth

H. C. BROOKES*, J. W. BAYLES, F. J. GRAHAM
Department of Chemistry, University of Natal, Durban 4001, South Africa

Received 31 August 1988; revised 9 May 1989

The influence of minor alloying elements (Mo, V, W) when added to a Fe18Cr alloy on the ability of a passive film to nucleate and grow on a freshly generated metal surface, and on the subsequent stability of the film was investigated as a function of electrolyte composition and applied potential using a scratch chronoamperometric technique. Mo and V decreased the rate of active dissolution prior to passivation, allowing the onset of passivation to occur more rapidly, and also improved the stability of the passive film, especially to attack by Cl^- in acidic (H_2SO_4, $HClO_4$) solutions. W additions had a detrimental effect on the repassivation behaviour of Fe18Cr. Repassivation of the scratch scars was evaluated, from the current transients, in terms of the number of layers of surface film formed.

1. Introduction

The passive film on stainless steel alloys, enriched in certain elements, influences the electrochemistry and corrosion properties of the substrate metal.

The structure of the passive film has been shown to be both potential and time dependent [1–5], and its composition is strongly dependent on the composition of the substrate alloy [6–9]. ESCA analysis of the passive films formed on austenitic and ferritic steels in neutral and acidic aqueous solutions has shown them to consist of an inner chromium rich oxide, nominally Cr_2O_3, and an outer mixed hydroxide layer (hydrated) containing Cr^{3+}, Fe and Mo (oxidation states of which are dependent on the potential of passive film formation) with the transition from the oxide to the hydroxide being continuous [4].

For a given bulk alloy chromium content, the addition of minor alloying elements, for example molybdenum, to a FeCr alloy results in higher concentrations of chromium being detected in the passive film of that alloy [10]. The beneficial influence of molybdenum is dependent on the concentration of chromium in the alloy [11–14], and the synergistic effect of these two elements has been well documented [15–18]. Thus the resistance to corrosion, especially pitting corrosion, is a complex non-linear function of both the chromium and molybdenum contents of the alloy, and while it is agreed that the addition of molybdenum to the alloy results in a stabilization of the passive film, the location, oxidation state and interaction of molybdenum with the other species within the film remains uncertain.

Available evidence indicates that the effect of molybdenum is not to be found in its enrichment in the passive film, but rather in changing the kinetics of anodic dissolution and passive film formation on the alloys. Olefjord *et al.* [19] suggested that the accumulation of the alloying elements (Mo and Cr) in the outermost layers of the alloy, during the active dissolution that preceeds passivation, results in a decrease in the dissolution rate, thereby promoting the formation of a passive film. In addition, Yaniv *et al.* [20] suggests that molybdenum improves the quality of the bonding at the metal/film interface by creating a barrier type oxide. This would explain the improved resistance of the molybdenum alloys to Cl^- induced pitting, since dissolution of the film would be more difficult and pit nucleation thus retarded.

Despite the advantages of including molybdenum as an alloying element in stainless steels, it is expensive. Substitution of molybdenum with a cheaper element is thus desirable. Possible substitutes have been considered [21], and vanadium appears to be an attractive alternative. It is for this reason that vanadium- and tungsten-containing superferritic stainless steels have been included in the present study.

Little has been published on the electrochemical and corrosion properties of FeCrV and FeCrW alloys or on the role of vanadium and tungsten in the passivation process.

The bulk of published work on the growth of passive films has been performed on either precathodized or preanodized electrodes. The former, reducing any oxide films present, has the disadvantage of producing hydrogen which may be adsorbed onto or absorbed into the electrode surface, and subsequently oxidized during anodization. Oxide films formed by preanodiz-

* To whom correspondence should be addressed.

0021-891X/90 $03.00 + .12 © 1990 Chapman and Hall Ltd.

ation may undergo rearrangement during subsequent applied potential or current programmes. Such investigations can only follow the final stages of film growth, as evident from the charge density ranges reported [22, 23]. However, a technique of rapid mechanical scratching of potentiostatically controlled metal electrodes provides a method of examining the electrochemical properties of their surfaces initially free from oxide films. It also enables film formation to be studied from the earliest stages of film nucleation. This scratch technique has been highly developed and extensively used by Burstein and co-workers [24, 25], who have applied it successfully to repassivation and film growth studies on iron and stainless steel type alloys.

In this paper the influence of potential and of the addition of minor alloying elements, namely molybdenum, vanadium and tungsten to a Fe18Cr alloy on the repassivation of a freshly generated metal surface was investigated using scratch chronoamperometric techniques in 0.1 M H_2SO_4 and $HClO_4$ solutions with and without Cl^- ions. This paper presents a phenomenological discussion of the scratch chronoamperometric results while a more quantiative analysis is presented in Part II.

2. Experimental

A dual working electrode assembly, similar to that described by Newman and Franz [26], was employed, with Fe18.5Cr as the one electrode and a FeCrMo, FeCrV or FeCrW alloy as the other. The advantage of this system is that it affords a significant degree of confidence in any comparisons made between the two electrodes, since the rate of scratch generation and the pressure of the diamond stylus on the electrodes will be the same.

For these experiments the working electrode consisted of two alloy strips (1 mm × 5 mm) set parallel to each other (~ 1 mm apart). The composition of the stainless steels used is given in Table 1. An insulated copper lead was secured to the back of each strip using a silver epoxy cement. The strips were mounted in Lecoset cold curing resin, and the epoxy mount press – fitted into a Teflon holder. The electrodes were polished to a 0.25 μm diamond paste finish. Electrochemical cleaning involved holding the electrodes at −1.0 V for 10 min, in either 0.1 M H_2SO_4 or 0.1 M $HClO_4$ (the bulk electrolyte) to reduce any air-formed oxide.

The electrolytes (0.1 M H_2SO_4 and 0.1 M $HClO_4$) were diluted from analytical grade reagents with ultrapure deionized water (Millipore-Q water purification system), and were deoxygenated with high purity nitrogen. NaCl was used for all Cl^- additions. Subsequent to Cl^- additions the solution was stirred with a magnetic stirrer and nitrogen bubbled through the solution to ensure homogeneity of the electrolyte.

For experiments having two working electrodes a six electrode cell was used, having a Pt disc and a Pt wire (spiral) counter electrodes and two mercurous sulphate reference electrodes. The two reference electrodes were frequently compared to ensure that $\Delta E_{RE1-RE2} = 0.00\,mV \pm 0.05\,mV$ and were changed when this criterion was not met. The reference electrodes were each placed in the electrolyte reservoir of a Luggin capillary. All quoted potentials are with respect to SSE. Each working electrode was controlled by a separate potentiostat (namely, WE1, CE1 and RE1 by a PAR 173; WE2, CE2 and RE2 by a PAR 363 programmed by a PAR 175). With the exception of the electrolyte there was no electrical connection between either working electrode system. The current response of the working electrodes was recorded on a dual channel digitizing oscilloscope (Nicolet 3091) and the data transferred to an Apple II+ computer for storage and processing.

A scratcher, consisting of a diamond set in an epoxy-coated brass rod, attached to a glass syringe plunger, was incorporated in the cell. At the commencement of an experiment, the height of the working electrode was adjusted so that the culet of the diamond just touched the working electrode surface. At the potential of interest, the scratcher was rapidly drawn across the width of both electrodes and the current responses recorded on the oscilloscope. The

Table 1. The chemical composition of the alloys (wt%)

Alloy element	*Cr*	*Mo*	*V*	*W*	*C*	*Ni*	*Annealing temp (°C)*	*Annealing period (min)*
Fe18.5Cr	18.29	0.011	0.009	–	0.03	0.02	800	120*
Mo containing								
444	17.39	1.78	0.081	–	0.003	0.27	850	15†
V containing								
4732	18.40	0.02	2.77	–	0.017	0.09	825	30†
4733	18.20	0.02	4.08	–	0.019	–	825	10†
W containing								
Fe18Cr3W	17.94	–	–	3.00	0.072	0.50	1200	60*
Fe17Cr6W	16.38	–	–	5.73	0.122	0.50	1200	60*

The balance in all the alloys is iron
– not measured
Subsequent to annealing the alloys were: * air cooled; † water quenched.

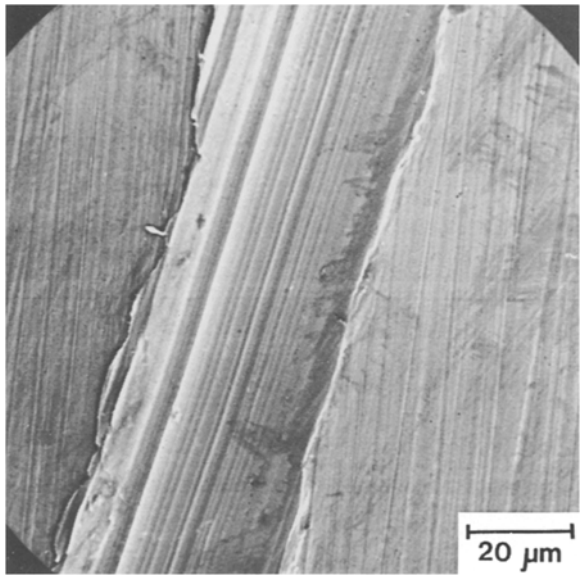

Fig. 1. SEM image of a section of a single scratch on a 444 alloy electrode.

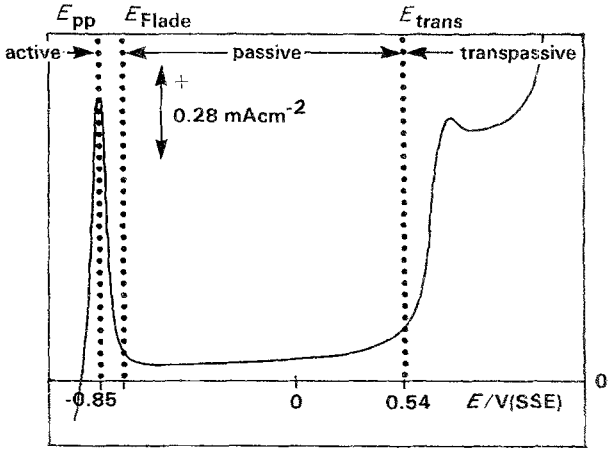

Fig. 2. Anodic polarization curve for a Fe18.5Cr alloy electrode in 0.1 M H_2SO_4 polarized between -1.00 and $+1.00$ V at 2 mV s^{-1}, showing the primary passivation potential (E_{pp}), the Flade potential (E_{Flade}), the transpassive potential (E_{trans}) and the active, passive and transpassive potential regions.

scratch scars were subsequently examined using a Japan Electron Optics Laboratory JSM-35 scanning electron microscope. The area of the scratch scars was determined from stereomicrographs.

A reproducible scratch technique was developed that ensured that the scratch depth was sufficient to remove the preformed passive film and expose a bare metal surface. Excellent reproducibility of the scratch depth and width were achieved (width, 35 $\pm$ 5 μm; depth, 40 $\pm$ 5 μm across the width of each electrode, typically 1 mm). A typical scratch scar is shown in Fig. 1.

For these experiments the electrodes were passivated at -0.1 V for five minutes then stepped to the potential of interest and, within two seconds, the surfaces of the electrodes were scratched. The electrodes were then repassivated at -0.1 V.

3. Results and discussion

The significance of the various potentials quoted in this article is indicated on the typical anodic polarization curve for the Fe18.5Cr alloy electrode in 0.1 M H_2SO_4 shown in Fig. 2.

3.1. *0.1 M H_2SO_4 + x M Cl^-*

Typical chronoamperometric responses of scratched electrodes in 0.1 M H_2SO_4 are shown in Fig. 3a, b. For all alloys investigated (444, 4732, 4733, Fe18.5Cr, Fe18Cr3W and Fe17Cr6W) the same trends were observed. While the maximum current density (i_{max}) subsequent to exposing a new surface by scratching decreased, the rate of current decay increased as the potential to which the electrodes were stepped was made more cathodic.

For a passive film to grow by ion conduction in the presence of a high electric field, it has been shown [25] that the anodic charge flowing from a newly generated metal surface goes exclusively into film formation with no significant dissolution occurring. It is also well established that the film thickness is a function of potential, with the thickness of the passive film being greater at the anodic end of the passive region than at the cathodic end [27]. Thus the decrease in the rate of current decay as the applied potential is made more anodic, as shown by the transients in Figs 3a and b, is due to an increasing rate of alloy dissolution at active potentials from -1.00 to -0.842 V (E_{pp} for Fe18.5Cr in 0.1 M H_2SO_4) and to passive film formation in the potential range -0.842 to 0.500 V (E_{pp} to E_{trans}). At potentials in the active region, and to a lesser extent in the active–passive transition region, a gradual increase (not shown) in current density was observed after the inital decay for alloys Fe18.5Cr, Fe18Cr3W and Fe17Cr6W when the current was recorded for up to 2 s after scratching. Such an increase was not observed at potentials in the passive region. At potentials cathodic to E_{Flade} any surface film present will not have the passivating properties of a film formed in the passive potential region, and there will be alloy dissolution. The subsequent increase in the active surface area of the electrode is responsible for this gradual increase in the current density.

At potentials in the transpassive potential region (> 0.500 V), transpassive dissolution of the passive film occurs. It is proposed that at transpassive potentials the current transients would also contain a dissolution component which would increase as the potential is made more anodic (0.500 to 1.200 V) and would account for the continuation of the trend whereby the rate of current decay decreases as the potential is made more anodic in the transpassive region. The marked increase in the current density at potentials anodic to 1.10 V (Fig. 3b) can be ascribed to the onset of oxygen evolution occurring at these potentials (cf. Fig. 2).

An exception to the above trend was observed in the potential region 0.00 to 0.30 V where the rate of current decay increases as the applied potential was made

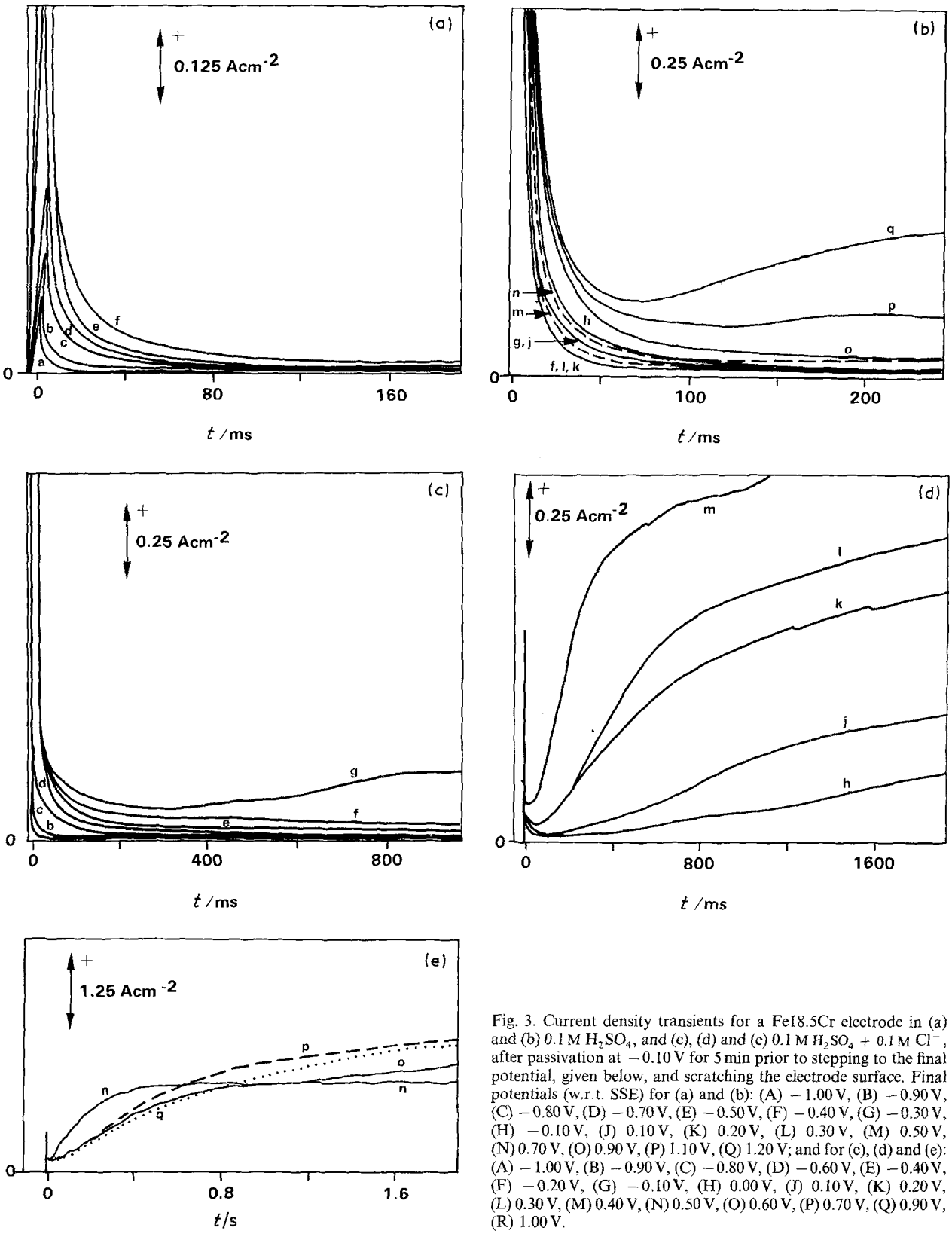

Fig. 3. Current density transients for a Fe18.5Cr electrode in (a) and (b) 0.1 M H_2SO_4, and (c), (d) and (e) 0.1 M H_2SO_4 + 0.1 M Cl^-, after passivation at −0.10 V for 5 min prior to stepping to the final potential, given below, and scratching the electrode surface. Final potentials (w.r.t. SSE) for (a) and (b): (A) −1.00 V, (B) −0.90 V, (C) −0.80 V, (D) −0.70 V, (E) −0.50 V, (F) −0.40 V, (G) −0.30 V, (H) −0.10 V, (J) 0.10 V, (K) 0.20 V, (L) 0.30 V, (M) 0.50 V, (N) 0.70 V, (O) 0.90 V, (P) 1.10 V, (Q) 1.20 V; and for (c), (d) and (e): (A) −1.00 V, (B) −0.90 V, (C) −0.80 V, (D) −0.60 V, (E) −0.40 V, (F) −0.20 V, (G) −0.10 V, (H) 0.00 V, (J) 0.10 V, (K) 0.20 V, (L) 0.30 V, (M) 0.40 V, (N) 0.50 V, (O) 0.60 V, (P) 0.70 V, (Q) 0.90 V, (R) 1.00 V.

more positive (Fig. 3b). In the potential region −1.00 to 0.00 V the increase in the charge subsequent to scratching the electrode may be attributed to the build up of the passive film, and at potentials anodic to 0.30 V to, initially, thickening of the passive film at the anodic limit of the passive region and to the onset of transpassive dissolution. It is proposed that the potential region 0.00 to 0.30 V is that in which the passive film is most stable since the increase in the rate of current decay suggests the more rapid attainment of the passive state.

Addition of Cl^- (0 to 0.1 M) to the electrolyte resulted in i_{max}, for a given potential, varying linearly with the chloride ion concentration and $di_{max}/d[Cl^-]$ varying linearly with applied potential (for the potential range −870 to 870 mV). At high Cl^- concentrations (0.1 M Cl^-) the initial current flow for the less corrosion resistant alloys (Fe18.5Cr, Fe18Cr3W and

Fe17Cr6W) did not decay to a steady state but increases as a function of time (Figs 3c (curve g), 3d, and 3e). At passive potentials the initial rate of this current rise increased as the final potential was made more anodic as shown in Fig. 3d. This rise is due to the commencement of pitting corrosion and the inability of the alloy to repassivate the pits. At transpassive potentials (Fig. 3e (curves O to R)) the magnitude of the increase in the current density after the initial decay was not very reproducible and thus no definite trends, with respect to applied potential as observed in the passive region, were evident within experimental error. This is due to the stochastic nature of pitting and the increased rate of pit nucleation and growth at transpassive potentials. At lower Cl^- concentrations (0.01 M) the same phenomenon was observed although the rate of current density increase was not as rapid.

i_{max} is a function of (i) speed of oscilloscope response, (ii) speed with which the scratch was made and (iii) the depth of the scratch. The experimental technique was developed to the extent that (ii) and (iii) were constant (SEM stereo-images were used to monitor (iii)). Thus with (i), (ii) and (iii) being constant for all experiments i_{max} should reflect the ease of dissolution of a particular alloy at a given potential and can therefore be used to make comparisons between alloys.

The addition of molybdenum and vanadium to a Fe18Cr alloy reduces i_{max} at active, passive and transpassive potentials, in 0.1 M H_2SO_4 in the presence of Cl^- up to 0.1 M. Tungsten additions reduce i_{max} of an Fe18Cr alloy held at passive potentials, and in the presence of Cl^-. However, at non-passive potentials addition of 3% W to a Fe18Cr alloy in 0.1 M H_2SO_4 results in an increase in i_{max}. Although 6% W reduced i_{max} it did not afford a stable passive film, since after two seconds, the chronoamperometric current density of both tungsten alloys increased. It should, however, be noted that while, for example, 2% Mo does not significantly reduce (by 3 to 9%) the initial rate of dissolution of the alloy, Mo and V do result in the onset of passivation occurring more rapidly (rate of current decay, after i_{max}, is greater for 444 than for Fe18.5Cr) and also improves the stability of the passive film once it has formed.

The effect of the addition of 1.78% Mo to a Fe18Cr alloy on the current transient response to scratching the electrode surface is shown in Fig. 4. In 0.1 M H_2SO_4 at −870 mV, the presence of molybdenum increases the rate of current decay subsequent to scratching, indicative of more rapid repassivation of the scratch – as shown by the faster attainment of steady state conditions by alloy 444 than by alloy Fe18.5Cr (Fig. 4a). At a passive potential, 0 mV, i_{max} for Fe18.5Cr is 1.5 × that of 444. Although the rate of decay is more rapid for the latter (Fig. 4b), both alloys attain the same current density two seconds after scratching the surface. Qualitatively, the same results are obtained when the electrode is stepped to transpassive potentials (Fig. 4c). These results indicate that molybdenum decreases the rate of active dissolution prior to passivation thus allowing the onset of passivation to occur more rapidly. Repassivation of the Fe18.5Cr scratch scar is achieved more slowly due to the longer period of active dissolution and the absence of molybdenum to assist with the repassivation of the scratch. Once passivation is achieved, molybdenum does not appear to further influence the growth of the passive film. These conclusions are supported by results from anodic polarization studies [28].

In the presence of Cl^-, at all potentials tested, i_{max} is not appreciably lower for the Mo-containing alloy. However, the rate of current decay after i_{max} is faster for 444 and the subsequent current density of the repassivated 444 scratch scar is lower and has fewer current fluctuations. Of greater significance is the fact that the current density of Fe18.5Cr starts to increase about 200 ms after scratching the electrode at −870 mV (Fig. 4d), and after 400 ms at 0 mV (Fig. 4e). This increase is particularly noticeable if the current transient is monitored for approximately two seconds after scratching. The current density of Fe18.5Cr continues to increase with time, indicating irreparable breakdown of the passive film and dissolution of the alloy. Subsequent SEM examination of the electrodes revealed the presence of pits on the Fe18.5Cr surface but not on the 444 surface. Thus the presence of molybdenum in an Fe18Cr alloy not only significantly improves the stability of the passive film to attack by Cl^-, but also increases the rate of repassivation (> 300 ms) of a surface defect, confirming the findings of Newman and Franz [26], and of Marshall and Burstein [29] for austenitic steels.

Similar experiments were performed using alloys 4732, 4733, Fe18Cr3W and Fe17Cr6W. The response of 4732 and 4733 (in comparison with Fe18.5Cr) was similar to that described for 444. However, tungsten additions to the Fe18Cr alloy had a detrimental effect on the corrosion resistance of this alloy, in that repassivation after scratching was slower (> 100 ms), than that of Fe18.5Cr, and at high Cl^- concentrations steady state current densities were not obtained owing to the continued increase in the current density as a result of pitting.

3.2. *0.1 M $HClO_4$ + x M Cl^-*

The above experiments were repeated using alloys 444 and Fe18.5Cr, and replacing 0.1 M H_2SO_4 with 0.1 M $HClO_4$. Qualitatively, the same trends were observed. However, for both alloys, i_{max} and the steady state current density after repassivation were greater than those observed in H_2SO_4; the magnitude of the increase was potential dependent as observed in 0.1 M H_2SO_4. This suggests that SO_4^{2-} and/or HSO_4^- have inhibiting properties. Another significant difference is that after the addition of 0.1 M Cl^- and on stepping alloy 444 from 0 to +870 mV, the current density did not decrease to a steady state value, but increased as a function of time after an initial current decay. Such an increase had not been observed with this alloy in 0.1 M H_2SO_4 which clearly indicates that the presence of ClO_4^- instead of SO_4^{2-} or HSO_4^- influences both the

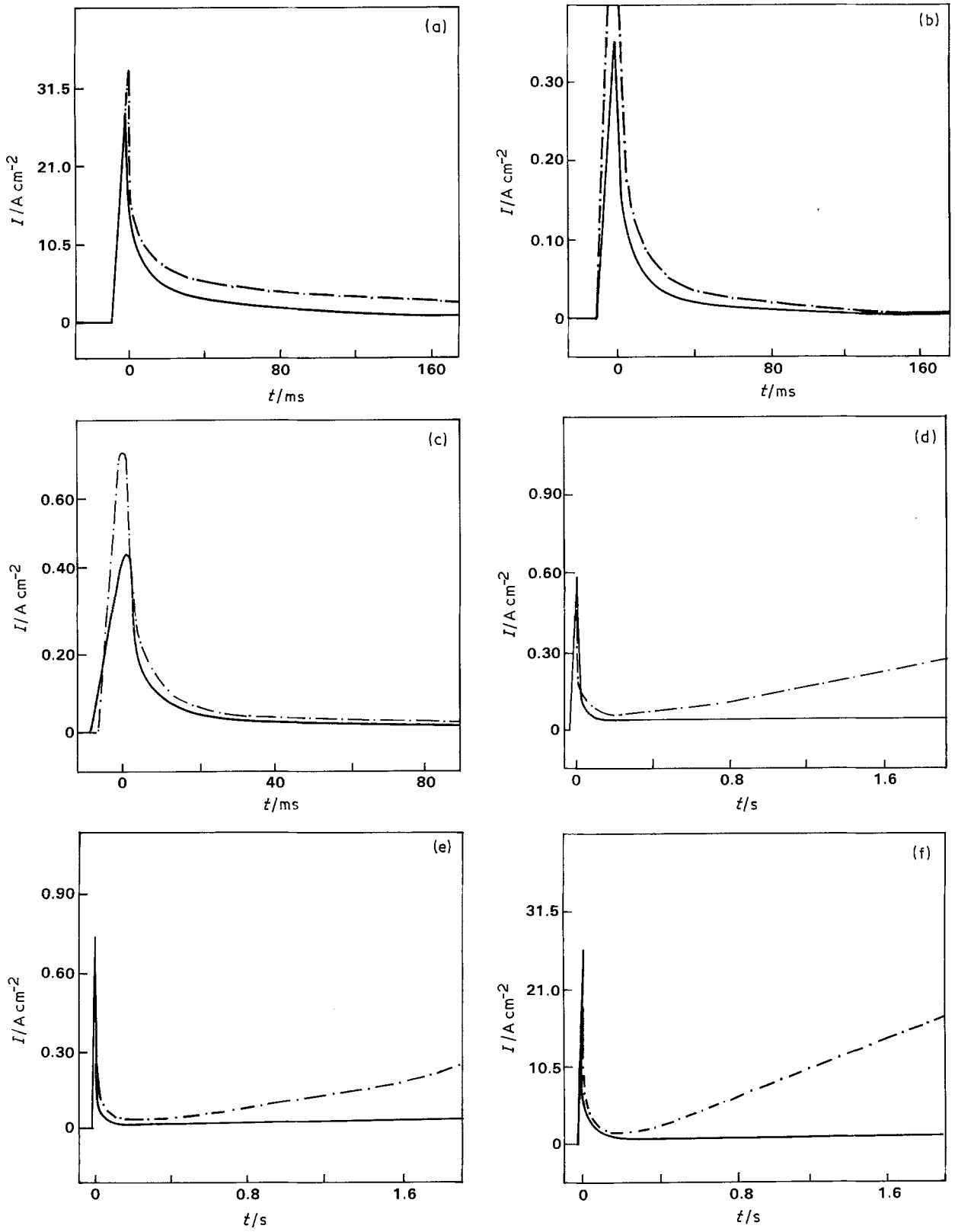

Fig. 4. Current density transients of alloys Fe18.5Cr (–·–·–) and 444 (——) in (a), (b) and (c) 0.1 M H_2SO_4 and (d), (e) and (f) 0.1 M H_2SO_4 + 0.1 M Cl^- after passivating the electrodes at −0.10 V for 5 min then stepping to (a) and (d) −0.870 V, (b) and (e) 0.000 V, and (c) and (f) +0.870 V and scratching the electrode surface.

ability of the alloy to repassivate and the stability of the anodic film.

3.3. *Evaluation of the repassivation of a scratch scar in terms of the number of monolayers of oxide formed*

For a given potential and electrolyte composition, the influence of molybdenum, vanadium and tungsten additions to a Fe18Cr alloy on the repassivation behaviour of this alloy was evaluated in terms of the charge required to repassivate the scratch scar with initial repassivation being taken as the onset of the steady state region subsequent to the initial current decay. Expression of this charge in terms of the number of layers of surface film assumed oxide, formed

Table 2. Charge required to inhibit active dissolution of a freshly generated metal surface, represented in terms of the number of oxide layers at the commencement of the steady state on the chronoamperograms of stainless steel alloys at specific potentials in (a) 0.1 M H_2SO_4 and (b) 0.1 M $HClO_4$, with varying chloride ion concentrations

	Alloy	E(mV)	Number of layers (±0.5)		
			$[Cl^-](M) = 0$	0.01	0.10
(a)	444	−870	1	1	2
	4733	−870	2	2	1
	4732	−870	1	2	2
	Fe18.5Cr	−870	5	8	7
	Fe18Cr3W	−870	2	5	8
	444	0	1	2	3
	4733	0	1	2	2
	4732	0	1	2	2
	Fe18.5Cr	0	2	3	5
	Fe18Cr3W	0	3	4	7
	444	+870	10	13	28
	4733	+870	11	12	30
	4732	+870	22	29	32
	Fe18.5Cr	+870	40	48	28
	Fe18Cr3W	+870	49	59	99
(b)	444	−870	1	2	2
	Fe18.5Cr	−870	1	3	80
	444	0	1	1	5
	Fe18.5Cr	0	4	6	22

(Table 2) can provide information regarding the initial passive film formed on repassivation.

3.3.1. 0.1 M H_2SO_4 + x M Cl^-. At 0 mV (a passivating potential) the values in Table 2 were calculated assuming a hexagonal close packed structure for Cr_2O_3 (with $n = 3$) since Cr^{3+} constitutes ~70% of the passive film [5]. It should, however, be noted that in the presence of Cl^- the passive film will become pitted, resulting in iron dissolution if repassivation of these pits does not occur. Insufficient confirmed quantitative data regarding the exact nature and quantity of Fe, Mo, V and W hydroxides in the outer layers of the passive film precludes incorporation of the variations in the passive film arising from these elements in the calculations. At −870 mV the predominating process will be iron dissolution. The values in Table 2, for this potential, were calculated assuming a cubic close packed structure for iron ($n = 2$). At +870 mV, as the transpassive dissolution rate increases, (in the presence of Cl^-, and for the less corrosion resistant alloys) although the passive film thickness of Cr_2O_3 decreases, and while some Fe_2O_3 may be present, the predominant process will again be iron dissolution. Determination of surface enrichment of the minor alloying elements, as calculated by Newman [26], is precluded because of the synergistic interaction of these elements with chromium [15–18].

At potentials near the primary passivation potential the charge, and hence the number of monolayers, required to ihibit dissolution of alloys 4733, 4732 was almost the same as that for 444 in 0.1 M H_2SO_4, with and without Cl^- present (Table 2) and was markedly less than that for Fe18.5Cr. Thus, in this potential region the addition of 1.78% Mo, 3.77% V and 4.08% V to an Fe18.5Cr alloy has a beneficial effect on the corrosion resistant properties of the latter. Although addition of 3% W to Fe18Cr has a beneficial effect in 0.1 M H_2SO_4, it has a detrimental effect subsequent to the addition of 0.1 M Cl^- to the electrolyte, appearing to exacerbate attack by Cl^-.

In the passive potential region, 2.77% and 4.08% V have a similar beneficial effect to 1.78% Mo on the Fe18.5Cr alloy in the presence of 0.1 M Cl^-, whilst 3% W again has a detrimental effect.

Within 2 s of scratching the electrodes held at transpassive potentials (+870 mV) complete repassivation of the scratch scar had not always been achieved. Thus, the values in Table 2, for 870 mV, should be regarded as a comparison, between the alloys, of the dissolution/repassivation of the scratch scar within the first 2 s subsequent to its generation. With respect to the quantity of charge passed within 2 s of scratching the electrode surface, the ability of the alloys to suppress transpassive dissolution decreases in the order:

$$444 > 4733 > 4732 \gg \text{Fe18.5Cr} > \text{Fe18Cr3W}$$

indicating that 1.78% Mo and V (2 and 4%) suppresses dissolution of a Fe18Cr alloy while 3% W enhances the dissolution.

3.3.2. 0.1 M $HClO_4$ + x M Cl^-. The repassivation behaviour of alloys Fe18.5Cr and 444 was also investigated in 0.1 M $HClO_4$. At potentials near E_{pp} (−870 mV) the number of surface layers found for alloy 444 in both H_2SO_4 and $HClO_4$, with and without Cl^- present, were very similar (Table 2). These were also the findings at passive potentials (for $[Cl^-] \leqslant 0.01$ M); at higher Cl^- concentrations (0.1 M) approximately double the charge density required for repassivation of the scratch scar in 0.1 M H_2SO_4 was required in 0.1 M $HClO_4$. Since sulphate ions have been reported [28, 30] to inhibit pitting to a greater extent than perchlorate ions it was expected that the scratch scar would have repassivated more rapidly in the SO_4^{2-} containing electrolyte, and at $Cl^- \geqslant 0.01$ M this was indeed the case. Only when alloy Fe18.5Cr was held at potentials near E_{pp} with $Cl^- < 0.01$ M was the charge density required for repassivation greater in the SO_4^{2-} containing electrolyte. At such potentials in the presence of higher Cl^- concentrations and at passive potentials a greater charge density was required in the ClO_4^- containing electrolyte, as expected due to the SO_4^{2-} being a better inhibitor.

In 0.1 M $HClO_4$, particularly in the presence of Cl^-, the current density continued to increase subsequent to scratching the surface of an electrode held at transpassive potentials (+870 mV) suggesting no permanent and effective repassivation of the scratch scar and probably the commencement and propagation of pitting.

4. Conclusion

While chromium appears to act as the main passivating agent, the addition of molybdenum and vanadium to an Fe18Cr alloy increases the rate of repassivation of a surface defect, and thereby enhances the resistance of the passive film to attack by Cl^-, and so decreases the dissolution of the alloy thus improving the corrosion resistance of the alloy. Tungsten additions had a detrimental effect on passive film nucleation and growth, in that repassivation of the scratch scar was slower, and at high Cl^- concentrations ($\geqslant 0.1$ M) a steady state current density was not obtained after the initial decay indicating instability of the passive film in the presence of Cl^- and the commencement of pitting corrosion.

The nature of the anions present in the bulk electrolyte also influenced the repassivation behaviour, with SO_4^{2-}/HSO_4^- having a greater inhibiting effect on alloy dissolution than ClO_4^-, and while initial repassivation of a scratch scar in $HClO_4$ was possible the stability of the passive film over longer periods of time (> 2 s) and particularly in the presence of high Cl^- concentrations (0.1 M) was inferior to a film formed in SO_4^{2-} containing electrolytes. It has been found that:

1. As the applied potential was varied between -1.00 and $+1.00$ V i_{max} increased while the rate of current decay decreased.

2. An exception to the above trend occurred in the potential region 0.00 to 0.30 V in which the stability of the passive film is the greatest.

3. Mo and V result in the onset of passivation occurring more rapidly and also improve the stability of the passive film.

4. Repassivation of scratch scars occurred more readily in SO_4^{2-}/HSO_4^- containing electrolytes.

Acknowledgements

We thank the Foundation for Research Development, the University Research Fund and Middelburg Steel and Alloys for financial support, and ISCOR for alloys.

References

[1] M. Frolicher, A. Hugot-Le Goff and V. Jovancicevic, in 'Passivity of Metals and Semiconductors' (edited by M. Froment), Elsevier, Amsterdam (1983) p. 85.
[2] T. Ohtsuka, K. Azumi and N. Sato, *ibid.*, p. 199.
[3] K. Doss, A. Brooks and C. Clayton, *Int. Cong. Met. Corr.* **1** (1984) 138.
[4] I. Olefjord and B. Brox, in 'Passivity of Metals and Semiconductors' (edited by M. Froment), Elsevier, Amsterdam (1983) p. 561.
[5] I. Olefjord, B. Brox and U. Jelvestam, *J. Electrochem. Soc.* **132** (1985) 2854.
[6] G. Okamoto, *Corros. Sci.* **13** (1973) 471.
[7] G. Okamoto, T. Shibata, *ibid.* **10** (1970) 371.
[8] N. A. Nielson and T. N. Rhodin, *Z. Electrochem.* **62** (1958) 707.
[9] S. C. Tjong, *J. Mater. Sci. Lett.* **4** (1985) 6.
[10] I. Olefjord, *Mater. Sci. Eng* **42** (1980) 161.
[11] L. L. Wikstrom and K. Nobe, *J. Electrochem. Soc.* **116** (1969) 525.
[12] D. E. Williams, C. Westcott and M. Fleischmann, *ibid.* **132** (1985) 1796.
[13] K. Sugimoto and Y. Sawada, *Corros. Sci.* **17** (1977) 425.
[14] J. Ambrose, in 'Passivity of Metals' (edited by R. P. Frankenthal, J. Kruger), Electrochem. Soc., Princeton, New Jersey (1978) p. 740.
[15] A. P. Bond, *J. Electrochem. Soc.* **120** (1973) 603.
[16] E. A. Lizlovs and A. P. Bond, *ibid.* **122** (1975) 719.
[17] M. A. Streicher, *Corrosion* **30** (1974) 77.
[18] R. Goetz and D. Landolt, *Electrochim. Acta* **29** (1984) 667.
[19] I. Olefjord, B. Brox and U. Jelvestam, *Proc. Electrochem. Soc.* **84-9** (1984) 388.
[20] A. E. Yaniv, J. B. Lumsden and R. W. Staehle, *J. Electrochem. Soc.* **124** (1977) 490.
[21] F. P. A. Robinson and P. van Biljon, *Corrosion* **41** (1985) 220.
[22] N. Sato and M. Cohen, *J. Electrochem. Soc.* **109** (1962) 781.
[23] H. Wroblowa, V. Brusic and J. O'M. Bockris, *J. Phys. Chem.* **75** (1971) 2823.
[24] J. Pattison and G. T. Burstein, *Proc. Electrochem. Soc.* **85-3** (1985) 108.
[25] G. T. Burstein and P. I. Marshall, *Corros. Sci.* **23** (1983) 125.
[26] R. C. Newman and E. M. Franz, *J. Electrochem. Soc.* **131** (1984) 223.
[27] G. Okamoto and T. Shibata, in 'Passivity of Metals' (edited by R. P. Frankenthal and J. Kruger), Electochem. Soc., Princeton, New Jersey (1978) p. 646; and references therein.
[28] H. Brookes and F. Graham, *Corrosion* **45** (1989) 287.
[29] P. I. Marshall and G. T. Burstein, *Corros. Sci.* **24** (1984) 463.
[30] H. P. Leckie and H. H. Uhlig, *J. Electrochem. Soc.* **113** (1966) 1262.